

# Large-scale optical interferometry in general spacetimes

Daniel R. Terno,<sup>1,2</sup> Giuseppe Vallone,<sup>3,4,5</sup> Francesco Vedovato,<sup>3,4</sup> and Paolo Villoriesi<sup>3,4</sup>

<sup>1</sup>*Department of Physics and Astronomy, Macquarie University, Sydney NSW 2109, Australia*

<sup>2</sup>*Shenzhen Institute for Quantum Science and Engineering,*

*Southern University of Science and Technology, Shenzhen 518055, P. R. China*

<sup>3</sup>*Dipartimento di Ingegneria dell'Informazione, Università degli Studi di Padova, Padova 35131, Italy*

<sup>4</sup>*Istituto Nazionale di Fisica Nucleare (INFN) — Sezione di Padova, Italy*

<sup>5</sup>*Dipartimento di Fisica e Astronomia, Università di Padova, via Marzolo 8, 35131 Padova, Italy*

We introduce a convenient formalism to evaluate the frequency-shift affecting a light signal propagating on a general curved background. Our formulation, which is based on the laws of geometric optics in a general relativistic setting, allows to obtain a transparent generalization of the Doppler frequency-shift without requiring to perform Local Lorentz transformations. It is easily applicable to stationary spacetimes, and in particular to the near-Earth experiments where geometry is described in the parametrized post-Newtonian approximation. We apply our recipe to evaluate the phase-shift arising in large-scale optical interferometric experiments, as the optical version of the Colella-Overhauser-Werner experiment.

## I. INTRODUCTION

Optical interferometry has been crucial in formulation and testing the special and general theories of relativity from the early times until present day [1–5]. Relative motion between the emitter and the detector, as well as propagation in a gravitational field, lead to changes in frequency — the Doppler effect and the gravitational red-shift, respectively — that are used in precision tests of relativity [4–9]. The kinematic and gravitational effects are often competing, and strenuous efforts are made to separate the effects of relative motion from pure gravitational effects in both frequency and phase measurements [8–12].

As long as the effects of quantum electrodynamics and/or quantum gravity are not important [13], the propagation of the electromagnetic field is governed by the appropriate classical wave equations on a fixed curved background [4, 14, 15]. For the minimally coupled electromagnetic field the vector potential  $A^\mu$  satisfies the linear equation

$$\square A^\mu - R^\mu{}_\nu A^\nu = 0, \quad (1)$$

where  $\square := \nabla^\mu \nabla_\mu$ , with  $\nabla_\mu$  the covariant derivative, and  $R^\mu{}_\nu$  is the Ricci tensor that are associated with the background metric  $g_{\mu\nu}$ .

The standard approach in classical and quantum optics [3, 16] is to describe the wave propagation by means of geometric optics and, if necessary, its corrections. These are derived by considering a decomposition of the vector potential as

$$\begin{aligned} A^\mu(x) &= e^{i\varpi\varphi(x)} \sum_{n=0}^{\infty} \varpi^{-n} \mathcal{A}_n^\mu(x) \\ &=: a^\mu e^{i\Phi} + e^{i\varpi\varphi(x)} \sum_{n \geq 1}^{\infty} \varpi^{-n} \mathcal{A}_n^\mu(x), \end{aligned} \quad (2)$$

where  $\varphi$  (and  $\Phi := \varpi\varphi$ ) are called the phase or the eikonal function, the amplitudes  $\mathcal{A}_n$  are slowly-varying on the appropriate scales and the large parameter  $\varpi$  is related to the peak frequency of the solution [3, 4, 15]. The eikonal and the amplitudes can be determined from the equations for the coefficients of the various  $\varpi^{-n}$  terms that are obtained by inserting

this vector potential into the wave equation and imposing the Lorentz gauge  $\nabla_\mu A^\mu = 0$ .

In this work our motivation is twofold. While the theory behind the calculation of the phase difference in optical interferometric experiments is long-established, not all of the implicit relations that are valid in a non-relativistic setting can be directly used in implementations that involve arbitrary motion in a curved spacetime. This is so even if the motion is slow and the spacetime is nearly flat, as in the regime of post-Newtonian approximation [17]. First, by using the invariance of phase under arbitrary coordinate transformations, we arrive to an explicit expression for the phase difference that is applicable in a general spacetime. This is essentially a re-statement of known results, but it is presented in a form that is particularly convenient for the post-Newtonian analysis.

As a corollary, we demonstrate how the frequency-shift, including the effects of both gravity and the relative motion, can be easily obtained. Both of these aspects are critical in satellite-based gravitational experiments, either in the LISA gravitational wave antenna [11] or in the proposed optical tests of the Einstein Equivalence Principle (EEP) [18, 19].

Our second goal is to present the conceptual basis for the interferometric red-shift experiment to test the EEP proposed in Ref. [20], where a Doppler-cancellation scheme isolating the desired gravitational effect is introduced.

This work is organized as follows. We summarize the necessary background and provide expressions for the evaluation of the phase in Sec. II. The frequency-shift is calculated in Sec. III, in two different settings, and its implications for large-scale optical interferometric experiments, as well as the key idea underlying the red-shift measurement proposal of Ref. [20] are analysed in Sec. IV.

*Notation.*—We label the coordinates of a spacetime point as  $x^\mu = (t, \vec{x})$ , where  $\vec{x}$  designates a triple of spacelike coordinates  $(x^1, x^2, x^3)$ . These are given in a “global” coordinate frame, in contrast to the other “local” reference frames (such as that of emitters, mirrors, detectors, etc.) that can be established, with the trajectories parametrized either by their proper time  $\tau^{\text{frame}}$  or by the global coordinate time  $t$ . We use the signature  $(-, +, +, +)$  for the metric. The quantity  $r := |\vec{x}| = \sqrt{(x^1)^2 + (x^2)^2 + (x^3)^2}$  always stands for length

of the Euclidean vector  $\vec{x}$ . Both co- and contravariant vectors on a three-dimensional curved space are designated by the boldface font, e.g.,  $\mathbf{k}$ . Unless stated otherwise we use  $G = c = 1$ .

## II. PHASE EVALUATION IN A RELATIVISTIC SETTING

*The laws of geometric optics.*—Within the domain of validity of geometric optics [3, 15] the wave vector

$$k_\mu := -\nabla_\mu \Phi \equiv -\partial_\mu \Phi = -\varpi \partial_\mu \varphi, \quad (3)$$

defines the propagation and the spatial periodicity of the wave. It is null (in all orders of the asymptotic expansion of Eq. (2)) and thus it satisfies the eikonal equation:

$$k^\mu k_\mu = \partial_\mu \Phi \partial^\mu \Phi = 0, \quad (4)$$

which is a restatement of the null condition in terms of the phase function. Taking the gradient of the null condition,  $\nabla_\mu (k \cdot k) = 0$ , results in the propagation equation for the wave vector, that is

$$k^\mu \nabla_\mu k^\nu = 0, \quad (5)$$

where the geodesic is affinely parameterised.

The three-dimensional hypersurfaces of constant  $\varphi$  are null. In the high-frequency limit  $\varpi \rightarrow \infty$ , these are the hypersurfaces of constant phase. The integral curves of  $k^\mu$  form a twist-free null geodesic congruence. These geodesics are the light rays of geometric optics. These rays can be also thought of as trajectories of fictitious photons that generate the hypersurface  $\Pi_\Phi$  of constant phase  $\Phi$  and at the same time are orthogonal to it due to Eq. (4) [4, 14]. The eikonal equation [Eq. (4)] is the Hamilton-Jacobi equation for massless particles on a given background spacetime. Its specific solution is determined by prescribing the phase on some initial spacelike hypersurface, e.g.,  $\Phi(t = t_0, \vec{x})$ . In the caustic-free domain the value of  $\Phi$  at some point  $(t, \vec{x})$  is obtained by tracing the geodesic that passes through it to the point on the initial hypersurface.

If we consider the vectorial nature of electromagnetic waves, the polarization vector is defined as  $f^\mu := a^\mu / \sqrt{a^\mu a_\mu^*}$ . It is transversal to the null geodesic generated by  $k^\mu$ , and the Lorentz gauge condition implies the parallel propagation equation for the polarization:  $f^\mu k_\mu = 0$  and  $k^\mu \nabla_\mu f^\mu = 0$ .

Solutions of the Hamilton-Jacobi equation are particularly simple in stationary spacetimes, where the metric tensor is independent of the time coordinate. In such spacetimes existence of the timelike Killing vector  $\partial_0$ , such that  $\partial_0 g_{\mu\nu} = 0$ , ensures that  $\omega_0 = -(k[t_0, \vec{x}_0])_0$  is constant along the geodesic.

If the frequency is fixed in the proper frame of a static observer then  $\omega_0$  has same value on all geodesics that emanate from  $\vec{x}_0$ . Given the orthonormal tetrad  $e_\mu^{(A)}$ ,  $A = 0, \dots, 3$ , the conserved frequency is

$$\omega_0 = -e_0^{(A)} k_A = \text{const}, \quad (6)$$

where  $k_A$  are components of the wave 4-vector in the proper frame of the observer. The 4-velocity of the observer defines its time axis. For a static observer in a stationary spacetime it is  $e^{(0)\mu} = \delta_0^\mu / \sqrt{-g_{00}}$ , and thus by orthogonality of the tetrad  $e_0^{(I)} = 0$ , for  $I = 1, 2, 3$ . As a result the conserved frequency depends only on the proper frequency and the metric.

Static observers follow the congruence of timelike Killing vectors  $\partial_0$  that defines a projection from the space-time manifold  $\mathcal{M}$  onto a three-dimensional space  $\Sigma_3$ . Using the Landau-Lifshitz formalism [21–23] the spacetime domain is foliated by the hypersurfaces of simultaneity  $\Sigma_3(t)$  with respect to the static observer. This time  $t$  is the universal time that we use below. The foliation introduces the time-independent spatial metric  $\gamma_{mn}$  that determines geometric properties of the three-dimensional space  $\Sigma_3$ .

The three coordinates of the point  $x^\mu = (x^0 = t, \vec{x}) \in \Sigma_3(t)$  are just the triple  $\vec{x} = (x^1, x^2, x^3)$ . Both spatial vectors and covectors on this space are obtained by simply retaining the spatial components, as  $\mathbf{k}^m = k^m$ , and  $\mathbf{k}_m = \gamma_{mn} \mathbf{k}^n \equiv k_m$ .

Intersection of the hypersurface of simultaneity  $\Sigma_3(t)$  with the hypersurface of the constant phase  $\Pi_\Phi$  results in the instantaneous two-dimensional surface  $\Pi_2(t; \Phi)$  of the constant phase of the wave front. While the four-vector  $k$  is tangent to the world line of a fictitious photon and orthogonal to the null hypersurface  $\Pi_\Phi$ , its three-dimensional projection  $\mathbf{k}$  is perpendicular to the surface of constant phase  $\Pi_2$  and tangent to the light ray in the space  $\Sigma_3$ . In static spacetimes the geodesic equation and the evolution equation of polarization can be conveniently written in a three-dimensional form [22, 23]. If  $(t, \vec{x})$  is connected to  $(t_0, \vec{x}_0)$  by a null geodesic, then the coordinate travel time depends only on the spatial coordinates via some function  $T(\vec{x}; \vec{x}_0)$  such that  $t - t_0 = T(\vec{x}; \vec{x}_0)$ .

Thus the leading term of the asymptotic expansion leads to the *three laws of geometric optics* [3, 4, 15]. Namely:

- (i) Fields propagate along null geodesics. In stationary spacetimes their propagation can be visualized as the advance of a two-dimensional surface of constant phase in three-dimensional space that is guided by the light rays.
- (ii) Polarization is parallel-transported along the rays.
- (iii) Intensity satisfies the inverse-area conservation law.

The superposition of two or more light waves results in the appearance of interference. Phases, intensities and polarizations of the individual waves are calculated in the approximation of geometric optics according to the above rules (i)-(iii).

*Phase evaluation.*—Consider now a single null geodesic segment that connects two points —  $(t_E, \vec{x}_E)$  and  $(t_D, \vec{x}_D)$  — belonging to two timelike trajectories which are parametrized by their respective proper times, as sketched in Fig. 1. One,  $s_{\text{det}}^\mu(\tau^{\text{det}})$ , represents a detector and the other,  $s_{\text{tx}}^\mu(\tau^{\text{tx}})$ , represents the transmitter. In the frame of the point-like transmitter, the phase of the emitted signal at the emission instant  $\tau_E^{\text{tx}}$  is  $\Phi_E(\tau_E^{\text{tx}})$  and can be written as

$$\Phi_E(\tau_E^{\text{tx}}) = -\omega_{\text{tx}}(\tau_E^{\text{tx}} - \tau_0^{\text{tx}}), \quad (7)$$

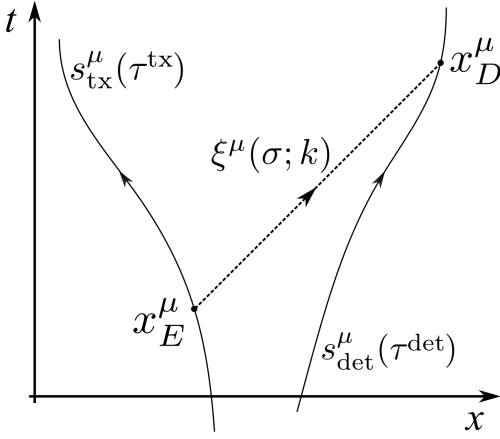


FIG. 1: A schematic representation of the world lines of the emitter (trajectory  $s_{tx}^\mu$ ), the detector (trajectory  $s_{det}^\mu$ ) and the light ray  $\xi^\mu$  between the emission event  $E$  and the detection event  $D$  (dotted straight line).

where we assume a constant proper frequency  $\omega_{tx}$  and  $\tau_0^{tx}$  determines the initial phase. We recall that the local frequency  $\omega_{fr}$  of the optical signal with wave vector  $k$  in some frame that is moving with the four-velocity  $u_{fr}^\mu$  ( $\tau^{fr}$ ) is  $\omega_{fr} = -u_{fr}^\mu k_\mu$ .

Since the optical phase is constant along a spacetime trajectory of the photon, the phase of the signal that is detected at the spacetime location  $x_D^\mu = s_{det}^\mu(\tau_D^{det})$  equals to the phase of the emitted signal at  $x_E^\mu$ . Given the detection at  $x_D^\mu$  of the signal with  $k^\mu$ , the coordinates of the emission event  $x_E^\mu = s_{tx}^\mu(\tau_E^{tx})$  are found as the intersection of the backward propagated geodesic from the detection point with the world-line of the emitter, that is

$$s_{tx}^\mu(\tau_E^{tx}) = \xi^\mu(\sigma; k). \quad (8)$$

where  $\sigma$  is the affine parameter and  $\xi^\mu(\sigma; k)$  is the spacetime trajectory of the photon. Using (i) the detected phase in terms of the properties of the emitter is given by

$$\Phi_D(\tau_D^{det}) = \Phi_E(\tau_E^{tx}(k)). \quad (9)$$

When it does not lead to confusion we simply write  $\tau_E \equiv \tau_E^{tx}$  and  $\tau_D \equiv \tau_D^{det}$  implying that we use the explicit form of the trajectories  $s_{tx}^\mu(\tau^{tx})$  and  $s_{det}^\mu(\tau^{det})$  to establish the relationship between the proper times of the emission and detection of a signal in the respective frames.

For a trajectory that consists of several geodesic segments the time procedure remains the same, but, in addition to the flight time, the phase changes at the nodes (such as  $\pi$  phases at the reflections) should be added to the final expression for the phase.

Consider now a two-beam interference where the beams arrive to the detector via two different paths. As not to clutter the expressions, we assume that the sums of the additional phases at the nodes of their respective trajectories are equal. Let the first and the second beams that arrive at  $x_D$  to have the wave vectors  $k_1$  and  $k_2$ , respectively. Then the phase difference at  $x_D$  is given by

$$\Delta\Phi(\tau_D) = \Phi_E(\tau_E(k_2)) - \Phi_E(\tau_E(k_1)), \quad (10)$$

where, in general,  $\tau_E(k_1) \neq \tau_E(k_2)$  due to the back-propagation, which is different for the two paths.

### III. FREQUENCY-SHIFT EVALUATION

#### A. Emission-Detection frequency-shift

The relationship between the observed frequency  $\omega_{det}$  and the proper frequency  $\omega_{tx}$  in the setting of Fig. 1 follows from our previous discussion. The constancy of the phase [Eq. (9)] leads to

$$\omega_{det} = -\frac{d\Phi_D}{d\tau_D} = -\frac{d\Phi_E}{d\tau_D} = \left(-\frac{d\Phi_E}{d\tau_E}\right) \frac{d\tau_E}{d\tau_D} = \omega_{tx} \frac{d\tau_E}{d\tau_D}. \quad (11)$$

In a general spacetime the relationship between the coordinate-times of emission and detection can be represented as

$$t_D(\tau_D) = t_E(\tau_E) + \mathbb{T}(s_{det}(\tau_D); s_{tx}(\tau_E)) \quad (12)$$

for some function  $\mathbb{T}$  that implicitly captures the relation between the proper time of emission and detection in the respective frames. Hence, on a generic background we obtain the frequency-shift by differentiating Eq. (12) and solving

$$\frac{dt_D}{d\tau_D} = \frac{dt_E}{d\tau_E} \frac{d\tau_E}{d\tau_D} + \frac{\partial\mathbb{T}}{\partial s_{det}^\mu} u_D^\mu + \frac{\partial\mathbb{T}}{\partial s_{tx}^\mu} u_E^\mu \frac{d\tau_E}{d\tau_D} \quad (13)$$

for  $d\tau_E/d\tau_D$ . Here the four-velocities are

$$u_D^\mu = \frac{ds_{det}^\mu}{d\tau_D}, \quad u_E^\mu = \frac{ds_{tx}^\mu}{d\tau_E}, \quad (14)$$

$$\frac{dt_D}{d\tau_D} = u_D^0, \quad \frac{dt_E}{d\tau_E} = u_E^0, \quad (15)$$

and the proper time is related to the coordinate time via

$$d\tau = \sqrt{|g_{00}| - g_{0k}v^k - g_{kl}v^k v^l} dt. \quad (16)$$

The above expression allows to evaluate the frequency-shift in a generic background by noting that Eq. (11) can be re-written as

$$\omega_{det} = \omega_{tx} \frac{d\tau_E}{dt_E} \frac{dt_E}{dt_D} \frac{dt_D}{d\tau_D}. \quad (17)$$

A more explicit expression is possible in a stationary spacetime, where Eq. (12) reduces to

$$t_D = t_E + T(\vec{x}_D; \vec{x}_E), \quad (18)$$

where  $T(\vec{x}_D; \vec{x}_E)$  is the interval of coordinate time that takes a null particle to travel from  $\vec{x}_E$  to  $\vec{x}_D$ , yielding

$$1 = \frac{dt_E}{dt_D} + \frac{\partial T}{\partial \vec{x}_D} \cdot \vec{v}_D + \frac{\partial T}{\partial \vec{x}_E} \cdot \vec{v}_E \frac{dt_E}{dt_D}. \quad (19)$$

For the near-Earth experiments the spacetime is well-approximated by the post-Newtonian expansion [4, 24, 25].

The parameterized post-Newtonian (PPN) formalism admits a broad class of metric theories of gravity, including general relativity as a special case. The key small parameter is  $\epsilon^2 \sim GM/c^2 r \sim v^2/c^2$ , where  $v$  is the velocity of a massive test particle or of some component of a gravitating body. The metric including the leading post-Newtonian terms (up to the second order in  $\epsilon$ ) is stationary and it is given by

$$g_{00} = -1 + 2U, \quad g_{ij} = \delta_{ij}(1 + 2U), \quad (20)$$

with  $U \equiv U(\vec{x}) := GMQ(r, \theta)/rc^2$  denoting the gravitational potential around the Earth, including the quadrupole term

$$Q(r, \theta) := 1 - \frac{1}{2}J_2 \frac{R^2}{r^2} (3 \cos^2 \theta - 1), \quad (21)$$

where  $J_2 = 1.083 \times 10^{-3}$  is the normalized quadrupole moment and the higher-order terms [26, 27].  $R$  is the Earth equatorial radius. Given the established bounds on the PPN parameter  $\gamma$  [5] we set  $(1 + \gamma) = 2$  in the metric.

For a spherically-symmetric Earth in the leading post-Newtonian expansion, the photon time-of-flight is given by [24, 25]

$$T^{\text{PPN}}(\vec{x}_D; \vec{x}_E) = T_0(\vec{x}_D; \vec{x}_E) + T_2(\vec{x}_D; \vec{x}_E), \quad (22)$$

where

$$T_0(\vec{x}_j; \vec{x}_i) := |\vec{x}_j - \vec{x}_i|, \quad (23)$$

is the flat spacetime result and the leading post-Newtonian term is

$$T_2(\vec{x}_j; \vec{x}_i) := 2M \ln \frac{r_j + \vec{x}_j \cdot \hat{n}_{ij}}{r_i + \vec{x}_i \cdot \hat{n}_{ij}}, \quad (24)$$

with  $r_i := |\vec{x}_i|$  the Euclidean length and

$$\hat{n}_{ij} := \frac{\vec{x}_j - \vec{x}_i}{|\vec{x}_j - \vec{x}_i|} = \frac{\vec{x}_j - \vec{x}_i}{r_{ij}} \quad (25)$$

is the Euclidean unit vector along the Newtonian propagation direction. For what follows, we note that

$$\frac{\partial T_0}{\partial \vec{x}_j}(\vec{x}_j; \vec{x}_i) = \hat{n}_{ij} = -\frac{\partial T_0}{\partial \vec{x}_i}(\vec{x}_j; \vec{x}_i). \quad (26)$$

We note that  $T^{\text{PPN}}(\vec{x}; \vec{x}_0)$  correctly satisfies (up to the second order in  $\epsilon$ ) the eikonal equation in Eq. (4) with the PPN metric of Eq. (20), i.e.,

$$\left| \frac{\partial T_0}{\partial \vec{x}}(\vec{x}; \vec{x}_0) \right|^2 = 1, \quad \frac{\partial T_0}{\partial \vec{x}}(\vec{x}; \vec{x}_0) \cdot \frac{\partial T_2}{\partial \vec{x}}(\vec{x}; \vec{x}_0) = 2U(\vec{x}). \quad (27)$$

Then, in the leading PPN approximation using Eq. (22) we obtain

$$\frac{dt_E}{dt_D} = \frac{1 - \hat{n}_{ED} \cdot \vec{v}_D - \frac{\partial T_2}{\partial \vec{x}_D} \cdot \vec{v}_D}{1 - \hat{n}_{ED} \cdot \vec{v}_E + \frac{\partial T_2}{\partial \vec{x}_E} \cdot \vec{v}_E} = \frac{1 - \hat{n}_{ED} \cdot \vec{v}_D}{1 - \hat{n}_{ED} \cdot \vec{v}_E} + \mathcal{O}(\epsilon^3). \quad (28)$$

and the PPN metric gives

$$d\tau = \sqrt{1 - 2U - v^2} dt + \mathcal{O}(\epsilon^4), \quad (29)$$

allowing to write, for example,

$$d\tau_E = \sqrt{1 - 2U_E - v_E^2} dt_E \quad (30)$$

so that at the second order in  $\epsilon$  we obtain the standard expression [9, 10, 27]

$$\frac{\omega_{\text{det}}}{\omega_{\text{tx}}} = \sqrt{\frac{1 - 2U_E - v_E^2}{1 - 2U_D - v_D^2}} \left( \frac{1 - \hat{n}_{ED} \cdot \vec{v}_D}{1 - \hat{n}_{ED} \cdot \vec{v}_E} \right) + \mathcal{O}(\epsilon^3) \quad (31)$$

for the frequency-shift. Using also the  $\epsilon^2$ -order time-delay term  $T_2$  [Eq. (24)] we obtain the frequency-shift that is valid up to  $\mathcal{O}(\epsilon^3)$ . Its explicit form is given in the Appendix.

## B. Emission-Reflection-Detection frequency-shift

In many practical situations, prior to the detection, the beam is reflected by a moving mirror. This is for example the case of the experiment realized in Ref. [28] and also the situation analyzed in Ref. [29]. We illustrate the analysis in this setting by considering the motion in a stationary spacetime. The path from the emission event  $E$  to the detection  $D$  now comprises two geodesic segments,  $E \rightarrow M \rightarrow D$ , where  $M$  stands for mirror.

Eq. (18) is now replaced by a pair of equations

$$t_D = t_M + T(\vec{x}_D; \vec{x}_M), \quad (32)$$

$$t_M = t_E + T(\vec{x}_M; \vec{x}_E), \quad (33)$$

that conveniently decompose the flight time  $t_D - t_E$ .

Now, the constancy of the phase allows to write

$$\omega_{\text{det}} = -\frac{d\Phi_D}{d\tau_D} = -\frac{d\Phi_M}{d\tau_D} = -\frac{d\Phi_E}{d\tau_D} = \omega_{\text{tx}} \frac{d\tau_E}{d\tau_D} \quad (34)$$

as in Eq. (11). The analogue to Eq. (17) now passes through  $M$  as

$$\omega_{\text{det}} = \omega_{\text{tx}} \frac{d\tau_E}{dt_E} \frac{dt_E}{dt_M} \frac{dt_M}{dt_D} \frac{dt_D}{d\tau_D}. \quad (35)$$

In the post-Newtonian approximation the two central ratios in the equation above are evaluated analogously to Eq. (28) by using Eqs. (32)-(33), yielding

$$\frac{dt_E}{dt_M} = \frac{1 - \hat{n}_{EM} \cdot \vec{v}_M}{1 - \hat{n}_{EM} \cdot \vec{v}_E} + \mathcal{O}(\epsilon^3) \quad (36)$$

$$\frac{dt_M}{dt_D} = \frac{1 - \hat{n}_{MD} \cdot \vec{v}_D}{1 - \hat{n}_{MD} \cdot \vec{v}_M} + \mathcal{O}(\epsilon^3) \quad (37)$$

and thus (up to  $\mathcal{O}(\epsilon^3)$ )

$$\frac{\omega_{\text{det}}}{\omega_{\text{tx}}} = \sqrt{\frac{1 - 2U_E - v_E^2}{1 - 2U_D - v_D^2}} \times \left( \frac{1 - \hat{n}_{EM} \cdot \vec{v}_M}{1 - \hat{n}_{EM} \cdot \vec{v}_E} \right) \left( \frac{1 - \hat{n}_{MD} \cdot \vec{v}_D}{1 - \hat{n}_{MD} \cdot \vec{v}_M} \right). \quad (38)$$



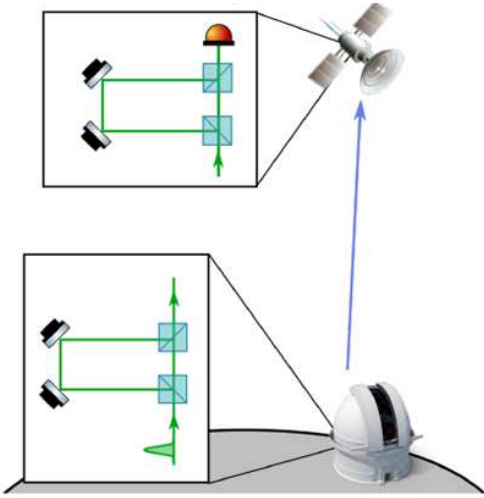


FIG. 2: Schematic representation of the interferometric red-shift measurement. For the stationary emitter and detector the only relevant effect is the difference in the coordinate time intervals that correspond to the same proper delay time  $\tau_l$ .

If the emission and detected occur at the same ground station then the first factor on the right-hand-side of above equation equals to unity.

#### IV. LARGE-SCALE OPTICAL INTERFEROMETRY

Measurements of the gravitational red-shift provide one of the fundamental tests of general relativity and metric theories of gravity in general [4, 5, 9, 24]. Possible violations of the equivalence principle (and, specifically of the assertion that outcomes “of any local non-gravitational experiment is independent of where and when in the universe it is performed” [5]) can occur as a result of a subtle interplay between different sectors of the Standard Model and its extension. Hence, a purely optical test provides a new type of a probe.

A basic version of the interferometric red-shift experiment (that tests the “where” part of the above assertion) [18, 19] is represented in Fig. 2, and it is known as the “optical-COW”, that is the optical version of the Colella-Overhauser-Werner experiment [30]. A light pulse is coherently split into two on the ground by using an interferometer of temporal imbalance  $\tau_l = l/c$ , with  $l$  the length of the optical delay line. The two pulses are recombined at the satellite by using another interferometer with the same imbalance  $\tau_l$ . Since the two interferometers sit at different gravitational potentials there will be a gravitational phase difference between the two interfering paths. It is estimated as

$$\varphi_{\text{gr}} = \frac{2\pi}{\lambda} \frac{ghl}{c^2}, \quad (39)$$

where  $g$  is the Earth’s gravity,  $h$  the satellite altitude and  $\lambda = 2\pi c/\omega$  the sent wavelength. Putting the emitter on a

ground-station (GS) and the detector on a low Earth orbit spacecraft (SC),  $\varphi_{\text{gr}}$  results of the order of few radians, supposing, as in Ref. [19], a delay of  $l = 6$  km,  $\lambda = 800$  nm and  $h = 400$  km. However, if the relative motion of the emitter and the detector is taken into account [17], then the first-order Doppler effect is roughly  $10^5$  times stronger than the desired signal  $\varphi_{\text{gr}}$ .

Here we provide a careful evaluation of the phase difference and show its relation to the frequency-shift. This analysis underlines the Doppler cancellation scheme that is proposed in Ref. [20]. The key events of the proposed experiment are depicted on Fig. 3.

Due to the Earth motion, the two pulses that recombine at the SC at the point  $D_2$  of the diagram leave the GS at two different times. The signal that took the short path in the GS-interferometer left the ground at  $\tau_{E_1}$ , while the pulse that took the long arm is delayed by  $\tau_l$  and departed at  $\tau_{E_2}$ . The interference condition at  $D_2$  and the back-propagations of the paths imply that the phase of the delayed pulse has to be evaluated at the instant  $\tau_C := \tau_{E_2} - \tau_l$ . Hence, the phase difference detected at the SC is

$$\Delta\Phi = \Phi_E(\tau_{E_1}) - \Phi_E(\tau_C) = -\omega_{\text{tx}}(\tau_{E_1} - \tau_C). \quad (40)$$

We will now show that for a sufficiently short proper delay time  $\tau_l$  the phase-shift in this scheme is proportional to the frequency difference  $\omega_{\text{det}} - \omega_{\text{tx}}$ . By defining  $\Delta\tau_E := \tau_{E_2} - \tau_{E_1}$ , we have that

$$\tau_{E_1} - \tau_C = \tau_l - \Delta\tau_E, \quad (41)$$

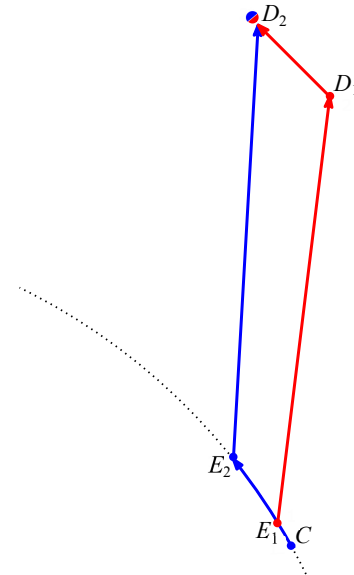


FIG. 3: Sequence of events in the experiment. The red line  $E_1D_1D_2$  represent the signal that was delayed on board of the SC, and the blue line  $CE_2D_2$  represents the signal that was delayed at the GS prior to transmission. The proper time intervals between the events  $D_1$  and  $D_2$  (at the SC) and  $C$  and  $E_2$  (at the GS) are both  $\tau_l$ .

and  $\Delta\tau_E$  can be found from the relation

$$\Delta\tau_E \approx \frac{d\tau_E}{d\tau_D} \Delta\tau_D, \quad (42)$$

with  $\Delta\tau_D := \tau_{D_2} - \tau_{D_1} \equiv \tau_l$ , where only the leading term in  $\tau_l$  is kept. Hence,

$$\begin{aligned} \Delta\Phi &= -\omega_{\text{tx}}(\tau_l - \Delta\tau_E) \\ &= \omega_{\text{tx}}\tau_l \left( \frac{d\tau_E}{d\tau_D} - 1 \right) \\ &\equiv (\omega_{\text{det}} - \omega_{\text{tx}})\tau_l, \end{aligned} \quad (43)$$

where the last equality follows from Eq. (11). This expression is the first-order approximation in  $\tau_l$  and is valid if both  $v_E \gg a_E(dt_E/d\tau_E)\tau_l$  and  $v_D \gg a_D(dt_D/d\tau_D)\tau_l$  hold, where  $a_E$  and  $a_D$  are accelerations of the GS and SC at the emission and the detection times, respectively. In the case of the PPN metric, the relation between  $\omega_{\text{det}}$  and  $\omega_{\text{tx}}$  can be obtained via Eq. (31).

## V. SUMMARY

Many of the implicit assumptions of the interferometry, such as relationships between distance and time, or even the logical consistency of the assumption that two interfering beams have the same central frequency, are not valid in the relativistic setting. However, the primary interpretation of the phase difference as arising from the difference in the emission times allows to obtain compact expressions that provide the conceptual basis for analysis of interferometric experiments in general spacetimes.

Constancy of the phase on propagating wave surfaces in the geometric optics approximation allows for a simple generalization of the Doppler effect to curved spacetimes. The resulting expression does not require transformations between reference frames for its use. In the limit of a short delay time the

phase shift in the proposed interferometric measurement of the gravitational red-shift is proportional to this frequency difference, confirming the original order of magnitude estimates and the unavoidable dominance of the first-order Doppler effect in the one-way interferometric red-shift experiment.

On the other hand, the first-order Doppler shift in the  $E \rightarrow M \rightarrow D$  case is twice the Doppler shift in  $E \rightarrow D$  case. This allows to eliminate the first-order Doppler effect in the interferometric measurements where two data sets (at the ground station and at the satellite) are produced, as proposed in Ref. [20].

## Acknowledgments

The work of DRT is supported by the grant FA2386-17-1-4015 of AOARD. Useful discussions with Alex Ling and Alex Smith are gratefully acknowledged. Fig. 3 was designed by Alex Smith.

## Appendix

The frequency-shift in Eq. (17) can be evaluated up to the order  $\mathcal{O}(\epsilon^3)$  by using the leading post-Newtonian correction to the time-of-flight as given by Eq. (22). Taking into account the dependence  $\hat{n}_{ED}$  that results in, e.g.,

$$\frac{\partial}{\partial \vec{x}_E} (\vec{x}_E \cdot \hat{n}_{ED}) = \hat{n}_{ED} \left( 1 + \frac{\vec{x}_E \cdot \hat{n}_{ED}}{r_{ED}} \right) - \frac{\vec{x}_E}{r_{ED}}, \quad (44)$$

$$\frac{\partial}{\partial \vec{x}_D} (\vec{x}_E \cdot \hat{n}_{ED}) = \frac{\vec{x}_E - (\hat{n}_{ED} \cdot \vec{x}_E)\hat{n}_{ED}}{r_{ED}} \quad (45)$$

$$\frac{\partial}{\partial \vec{x}_E} (\vec{x}_D \cdot \hat{n}_{ED}) = \frac{-\vec{x}_D + (\hat{n}_{ED} \cdot \vec{x}_D)\hat{n}_{ED}}{r_{ED}} \quad (46)$$

$$\frac{\partial}{\partial \vec{x}_D} (\vec{x}_D \cdot \hat{n}_{ED}) = \hat{n}_{ED} \left( 1 - \frac{\vec{x}_D \cdot \hat{n}_{ED}}{r_{ED}} \right) + \frac{\vec{x}_D}{r_{ED}} \quad (47)$$

we have

$$\frac{\partial T_2}{\partial \vec{x}_D} = \frac{2M}{r_{ED}} \left( \frac{\vec{x}_D \left( 1 + \frac{r_{ED}}{r_D} \right) + (r_{ED} - \vec{x}_D \cdot \hat{n}_{ED})\hat{n}_{ED}}{r_D + \vec{x}_D \cdot \hat{n}_{ED}} - \frac{\vec{x}_E - (\vec{x}_E \cdot \hat{n}_{ED})\hat{n}_{ED}}{r_E + \vec{x}_E \cdot \hat{n}_{ED}} \right) + \mathcal{O}(\epsilon^3), \quad (48)$$

and

$$\frac{\partial T_2}{\partial \vec{x}_E} = \frac{2M}{r_{ED}} \left( \frac{-\vec{x}_D + (\vec{x}_D \cdot \hat{n}_{ED})\hat{n}_{ED}}{r_D + \vec{x}_D \cdot \hat{n}_{ED}} + \frac{\vec{x}_E \left( 1 - \frac{r_{ED}}{r_E} \right) - (r_{ED} + \vec{x}_E \cdot \hat{n}_{ED})\hat{n}_{ED}}{r_E + \vec{x}_E \cdot \hat{n}_{ED}} \right) + \mathcal{O}(\epsilon^3). \quad (49)$$

Hence, the  $\mathcal{O}(\epsilon^3)$  term in Eq. (31) is

$$\delta^{(3)} = -\frac{\partial T_2}{\partial \vec{x}_D} \cdot \vec{v}_D - \frac{\partial T_2}{\partial \vec{x}_E} \cdot \vec{v}_E + (\vec{v}_E \cdot \hat{n}_{ED})^3. \quad (50)$$

- 
- [1] A. A. Michelson and E. W. Morley, *On the relative motion of the Earth and the luminiferous ether*, *Am. J. Science* **34** (203), 333 (1887).
- [2] LIGO Scientific Collaboration and Virgo Collaboration, *Observation of gravitational waves from a binary black hole merger*, *Phys. Rev. Lett.* **116**, 061102 (2016).
- [3] M. Born and E. Wolf, *Principles of Optics*, 7th ed., (Cambridge University Press, Cambridge, England, 1999).
- [4] C. W. Misner, K. S. Thorn, and J. A. Wheeler, *Gravitation*, (Freeman, San Francisco, 1973).
- [5] C. M. Will, *The Confrontation between General Relativity and Experiment*, *Living Rev. Relativity* **17**, 4 (2014)
- [6] H. E. Ives and G.R. Stilwell, *An experimental study of the rate of a moving atomic clock*, *J. Opt. Soc. Am.* **28**, 215 (1938).
- [7] R. V. Pound and G. A. Rebka, Jr., *Apparent Weight of Photons*, *Phys. Rev. Lett.* **4**, 337 (1960).
- [8] N. Ashby, T. E. Parker, and B. R. Patla, *A null test of general relativity based on a long-term comparison of atomic transition frequencies*, *Nature Phys.* **14**, 822-826 (2018).
- [9] R. F. C. Vessot, M. W. Levine, E. M. Mattison, E. L. Blomberg, T. E. Hoffman, G. U. Nystrom, B. F. Farrel, R. Decher, P. B. Eby, C. R. Baugher, J. W. Watts, D. L. Teuber, and F. D. Wills, *Test of relativistic gravitation with a Space-borne hydrogen maser*, *Phys. Rev. Lett.* **45**, 2081 (1980).
- [10] R. F. C. Vessot and M. W. Levine, *Gravitational redshift space-probe experiment*, *NASA technical report NASA-CR-161409*, 1979).
- [11] K. Danzmann and the LISA study team, *LISA: laser interferometer space antenna for gravitational wave measurements*, *Class. Quantum Grav.* **13**, A247 (1996).
- [12] M. Tinto and S. V. Dhurandhar, *Time-Delay Interferometry*, *Living Rev. Relat.* **17**, 6 (2014)
- [13] G. M. Shore, *Quantum gravitational optics*, *Contemp. Phys.* **44**, 503 (2003).
- [14] Y. Ueno, *On the wave theory of light in general relativity, I: path of light*, *Progress of Theoretical Physics* **10**, 442 (1953).
- [15] A. I. Harte, *Gravitational lensing beyond geometric optics: I. Formalism and observables*, *Gen. Relat. Gravit.* **51**, 14 (2019).
- [16] L. Mandel and E. Wolf, *Optical Coherence and Quantum Optics*, (Cambridge University Press, Cambridge, England, 1999).
- [17] A. Brodutch, A. Gilchrist, T. Guff, A. R. H. Smith, D. R. Terno, *Post-Newtonian gravitational effects in optical interferometry*, *Phys. Rev. D* **91**, 064041 (2015).
- [18] M. Zych, F. Costa, I. Pikovski, and Č. Brukner, *Quantum interferometric visibility as a witness of general relativistic proper time*, *Nature Commun.* **2**, 505 (2011).
- [19] D. Rideout, T. Jennewein, G. Amelino-Camelia, T. F. Demarie, B. L. Higgins, A. Kempf, A. Kent, R. Laflamme, X. Ma, R. B. Mann, E. Martín-Martínez, N. C. Menicucci, J. Moffat, C. Simon, R. Sorkin, L. Smolin and D. R. Terno, *Fundamental quantum optics experiments conceivable with satellites-reaching relativistic distances and velocities*, *Class. Quantum Grav.* **29**, 224011 (2012).
- [20] D. R. Terno, F. Vedovato, M. Schiavon, A. R. H. Smith, P. Magnani, G. Vallone, and P. Villoriesi, *Proposal for an optical test of the Einstein Equivalence Principle*, *arXiv: 1811.04835* (2018).
- [21] L. D. Landau and E. M. Lifshitz, *The Classical Theory of Fields*, (Butterworth-Heinemann, Amsterdam, 1980).
- [22] F. Fayos and J. Llosa, *Gravitational effects on the polarization plane*, *Gen. Relativ. Gravit.* **14**, 865 (1982).
- [23] A. Brodutch and D. R. Terno, *Polarization rotation, reference frames, and Machs principle*, *Phys. Rev. D* **84**, 121501(R) (2011).
- [24] C. M. Will, *Theory and Experiment in Gravitational Physics*, (Cambridge University Press, 1993)
- [25] E. Poisson and C. W. Will, *Gravity: Newtonian, Post-Newtonian, Relativistic*, (Cambridge University Press, 2014).
- [26] G. Schubert and R. L. Walterscheid, *Earth*, in A. N. Cox (ed.), *Allen's Astrophysical Quantities*, 4th edition, (Springer, New York, 2002), p. 239.
- [27] N. Ashby, *Relativity in GNSS*, in A. Ashtekar and V. Petkov (eds.), *Springer Handbook of Spaceime* (Springer, Berlin, 2014), p. 509.
- [28] G. Vallone, D. Dequal, M. Tomasin, F. Vedovato, M. Schiavon, V. Luceri, G. Bianco and P. Villoriesi, *Interference at the single photon level along satellite-ground channels*, *Phys. Rev. Lett.* **116**, 253601 (2016).
- [29] M. Rakhmanov, *Reflection of light from a moving mirror: derivation of the relativistic Doppler formula without Lorentz transformations*, *arXiv:physics/0605100* (2006).
- [30] R. Colella, A. W. Overhauser, and S. Werner, *Observation of gravitationally induced quantum interference*, *Phys. Rev. Lett.* **34**, 1472 (1975).